Check for updates

Preparation, Optimization, Characterization, and Evaluation of Rosuvastatin Loaded Solid Lipid Nanoparticles Using Quality by Design Approach

Nilesh B Chaudhari[*1] iD , Amar G Zalte[2] and Vishal S Gulecha[3]

[1,2] *Department of Pharmaceutics, School of Pharmaceutical Sciences, Sandip University, Nashik, India*

[3] *Department of Pharmacology, School of Pharmaceutical Sciences, Sandip University, Nashik, India*

Abstract: The present research work aims to prepare and characterize solid lipid nanoparticles (SLN) containing rosuvastatin calcium (RT). We aim to use a novel microwave-assisted microemulsion technique to produce Rosuvastatin-loaded SLN. The characterization of the optimized formulation of RTSLN was carried out by employing Fourier-transformed infrared spectroscopy (FTIR) and Differential scanning calorimetry (DSC) studies showed that there was no chemical interaction between drug (Rosuvastatin Calcium) and lipid (GMS), XRD indicated the amorphization of RTSLN formulation. In contrast, scanning electron microscopy (SEM) studies indicated that Rosuvastatin Calcium loaded SLNs are spherical, discrete, and homogeneous. In *vitro* and *ex vivo* drug release studies showed sustained drug release action. The effect of dependent variables such as entrapment efficiency (EE), particle size, and independent variables like % GMS and Poloxamer 407 was observed using a 3^2-factorial design approach. Optimized formulation was selected based on the 2D & 3D counter and surface response plots. The prepared formulations show percentage entrapment efficiency within the range of 53 to 78%, particle size in the 254.2 to 863.4 nm, and *in vitro* drug release was found to be 79.8%. Also, *ex vivo* absorption was 76.7 % for 8 hours. The need of the research work is to use microwave energy over conventional heating to prepare SLNs also helps to resolve problems associated with conventional colloidal drug delivery systems, which leads to improved drug bioavailability.

Keywords: Rosuvastatin calcium, solid lipid nanoparticles, microwave-assisted synthesis, controlled release, 3^2 Full-factorial design.

*Corresponding Author

Nilesh B Chaudhari , Department of Pharmaceutics, School of Pharmaceutical Sciences, Sandip University, Nashik, India

1. INTRODUCTION

Numerous research teams are investigating the viability of using SLN as a delivery system. To resolve the formulation problems like non-biodegradability and instability with conventional colloidal drug delivery systems, SLN gained great interest. To increase bioavailability and achieve sustained drug delivery[1], SLN is frequently employed. The Pharmacokinetics aspect of rosuvastatin calcium shows low aqueous solubility since it has crystalline nature and poor oral bioavailability of about 20% due to first-pass hepatic metabolism. Biochemical reactions like oxidation, lactonization, and glucuronidation of the liver metabolize Rosuvastatin. Principally, the metabolites are eliminated by biliary secretion[2]. An aspect of Rosuvastatin (RT) includes lowering the increased levels of total cholesterol since it is a specific and competitive inhibitor of HMG CoA reductase[3] as RT falls under the BCS class II drug, creating formulation challenges in making oral dosage form. In addition, it creates variance in the drug's bioavailability by causing varying drug dissolution and absorption in the gastrointestinal tract[4]. Thus, there is a need to develop a formulation of RT that increases oral bioavailability. One of the most well-known methods for increasing the bioavailability of highly lipophilic molecules is to employ lipid-based drug carriers[5]. Extensive research revealed that high potential is observed in lipid-based formulations to improve drug bioavailability and therapeutic drug efficacy via various mechanisms, namely increasing luminal solubilization, bypassing first-pass metabolism of the drug, and inhibiting the Cytochrome P450[6]. This article used a novel method to prepare SLN: the microwave-assisted microemulsion technique. To overcome the drawbacks associated with the conventional conduction heating method, which is employed in the microemulsion method of SLN preparation. Microwaves are photons at the lower end of the spectrum of electromagnetic radiation. Microwave consists of oscillating electric and magnetic field that travels at right angles to each other in the form of photons[6]. Microwave heating is dependent on dielectric heating. It's a property of a microwave to couple with reaction molecules in the vessel directly and increases temperature rapidly. Instant superheating (localized) is achieved due to dipole polarization[7]. Lipid nanoparticles like SLN are prepared using lipids and surfactants. These offer advantages like higher surface area, increased interface, more bioavailability and absorption due to increased solubility[7], drug targeting, and more half-life[8]. Which ultimately results in lower drug dose, toxicity, and improved safety and protection to non-targeted tissues[9,10]. A few limitations of SLN formulations are limited to drug loading, particularly for drugs with low aqueous solubility[10,11]. The present study focuses on formulating and optimizing RTSLN using a novel microwave-assisted microemulsion method[12], where an aqueous surfactant phase containing poloxamer 407 is mixed with a lipid phase containing glyceryl monostearate (GMS). Quality by design is a scientific way to finalize the formulation controls; hence 3^2 full factorial design was used to optimize SLN. EE, particle size, FTIR, DSC, XRD, SEM, in vitro, and ex vivo drug release were used to characterize optimized SLN formulation.

2. MATERIALS AND METHODS

2.1. Materials

A gift sample of Rosuvastatin calcium was obtained from Enaltec Labs PVT Limited, Mumbai, India, and Poloxamer 407 was provided as a gift sample by Corel Pharma, Ahmedabad. In addition, Glyceryl Monostearate has been purchased from Research lab fine chem, Mumbai. All other reagents and solvents used for the research study were of analytical grade.

2.2. Methods

2.2.1. Selection of lipid

The lipid in which the active ingredient has the highest solubility is selected. Therefore, the solubility of Rosuvastatin calcium was determined in different lipids such as glyceryl monostearate, stearic acid, and gelucire. In this determination, accurately weighed Rosuvastatin calcium was transferred in melted lipids until the clear and transparent solution was obtained[13].

2.2.2. Selection of Surfactant

Poloxamer 188, poloxamer 407, and various grades of tween and span were examined for appropriate selection of surfactant[14].

2.2.3. Preformulation studies

2.2.4. Determination of Rosuvastatin calcium solubility

Solvents such as water, ethanol, methanol, phosphate buffer pH 6.8, and chloroform were used to determine the solubility of Rosuvastatin. An accurately weighed quantity of drugs was transferred to the above solvents with continuous stirring. A UV spectrophotometer was used to determine solubility.

2.2.5. Determination of melting point

Digital melting point apparatus was used to determine the RT melting point.

2.2.6. Standard calibration curve of RT

Rosuvastatin calcium 10 mg was weighed and dissolved in 100 ml methanol. One ml of this solution was further diluted to 10 ml with methanol to get a 10 μg/ml methanolic solution of Rosuvastatin calcium. Aliquots of this solution were scanned between 200 to 400 nm in a UV – Visible spectrophotometer to get the absorption spectrum. The λmax value was noted and compared with that reported in the literature.

2.2.7. Method of Preparation

RTSLN was prepared by a novel microwave-assisted microemulsion technique followed by probe sonication. First, GMS was melted above its melting point in a microwave oven with a power of 320W. Continuous stirring was used to dissolve Rosuvastatin calcium in the lipid (molten state), after which Poloxamer 407 aqueous surfactant solution was added. The aqueous phase with Poloxamer 407 was also maintained at a similar temperature as that of the molten lipid phase. Then, the aqueous phase was added slowly into the hot oil phase. The resulting dispersion was constantly stirred (temperature was maintained above the melting point of GMS) until it got a clear microemulsion. After that, the hot oil in water (o/w) microemulsion was added to cold water at 2-4 °C which was stirred with a magnetic stirrer to obtain SLN. Formulated SLN was sonicated for 20 min, with probe

sonicator (PCI analytics)[15,16]. A resulting colloidal dispersion of SLN was cooled at room temperature and lyophilized. Southern Scientific freeze dryer was used to get the lyophilized product. The Lyophilization procedure was initiated after 24 hrs of refrigeration of formulation. The freeze-drying of formulation was performed at -40°C and under 0.5 lbs pressure[17,18].

2.2.8.   *Factorial experimental design for optimization*

Design Expert® 13 (state ease Inc, Minneapolis) software was employed to investigate the impact of formulation variables. A 3^2-full factorial optimization design was used with 13 randomized trial runs, including two factors and three levels. The lipid concentration (X1) and surfactant concentration (X2) were independent variables. However, % Entrapment efficiency (Y1) and particle size (nm) (Y2) as dependent variables or responses (Table I). 2D plots & 3D Counter surface response plots were designed to analyze the effect of independent variables. Version 13 of Design Expert software was used to fit the obtained data and analyze ANOVA. Collected data was also investigated to respond to surface methodology to explain the effects of concentration of lipid and surfactant on the dependent variable. Table I indicates 13 batch runs of RTSLN prepared using 3^2 full factorial designs[19]. The optimized formulation of RTSLN was selected for further characterization, viz. particle size, EE, FTIR, DSC, XRD, SEM, *in vitro*, and *ex vivo* drug release study.

Table I: A 3^2 full factorial optimization design with independent and dependent variables of RTSLN				
	Independent Variable		**Dependent Variable**	
Experimental Run	**% GMS (Lipid) X1**	**% Poloxamer 407 (Surfactant) X2**	**% Entrapment efficiency Y1**	**Particle Size nm Y2**
RT 1	-1	+1	68±1.53	553±2.52
RT 2	+1	-1	69±1.73	460.3±1.15
RT 3	0	0	62±1.53	590.1±2.90
RT 4	0	0	63±2.08	589.2±2.85
RT 5	-1	0	60±1.53	730.3±3.04
RT 6	+1	+1	78±2.08	254.2±2.08
RT 7	0	-1	58±2.52	760.4±1.00
RT 8	0	0.5	70±3.06	480.5±2.52
RT 9	-1	-1	53±2.65	863.4±2.04
RT10	+1	0	73±1.53	390.2±2.25
RT 11	0	0	61±4.04	592.4±1.73
RT 12	0	0	64±2.08	593.5±1.53
RT 13	0	0	60±1.73	588.6±2.31

Coded values of the independent variables			
Independent variable	**Low level(-1)**	**Low level(0)**	**Low level(+1)**
X1=% of GMS	1	3	5
X2= % of poloxamer 407	0.1	0.3	0.5

2.3.   *Characterization*

2.4.   *Entrapment Efficiency*

Ultracentrifugation is subjected at 10,000 rpm for 1 hour to separate or settle the drug-loaded SLN from the dispersion. To solubilize the lipid of SLN, pour 5 ml of chloroform into the separated samples of SLN, which resulted in lipid precipitation. Moreover, chloroform was removed by evaporation to dryness. Add methanol and bath sonicate for 10 min. Finally, filter through Wattman filter paper (0.45 μm). Dilute with methanol if necessary. Measured the absorbance at 242.5 nm, and the concentration of Rosuvastatin calcium was calculated using the calibration equation. The amount of drug was calculated using the dilution factor[19,20].

$$\% \ Entrapment \ Efficiency = \frac{The \ actual \ amount \ of \ drug \ entrapped \ in \ SLN}{The \ total \ amount \ of \ drug \ added \ in \ SLN} \times 100$$

2.5.   *Particle size*

To determine the particle size of RT-loaded SLN liquid samples, a nano plus particulate system instrument was used to find out particle size[2]. The average particle size and size distribution of each rosuvastatin solid lipid nanoparticle dispersion were recorded[19,20].

2.6.   *Zeta potential and polydispersity index*

Double distilled water was used to disperse freeze-dried nanoparticles. Zeta potential was measured using a Particulate System; Nanoplus zeta/nanoparticle analyzer photon correlation spectroscopy is the main principle for particle size measurement. The polydispersity index (PDI) was used to study to determine the particle size distribution. Zeta potential was used to study the surface charge of SLNs. The zeta potential was studied with the help of electrophoretic light scattering (ELS) at 25 °C with an electric field strength of 23 V/cm using the NanoPlus Particulate System. All the measurements were taken out in triplicate.

2.7.   *Fourier transforms Infrared spectroscopy (FTIR)*

Shimadzu FTIR-8400 was used to record the IR spectra of RT and the RT SLN. The sample disc was prepared by mixing a sample of RT and RTSLN with KBr and compressing it using a KBr press. A range of wave numbers 4000 to 400 cm^{-1} was used to examine transmission[19,20].

2.8.   Differential Scanning Calorimetry

DSC 3 Star system, Mettler Toledo, was used to record the DSC thermogram of RT. 20 ml/min Nitrogen flow at a scanning rate of 100c/min. It was used to analyze the samples in sealed aluminum pans[20,21].

2.9.   X-ray diffraction (XRD) analysis

A Bruker AXS Advance D-8 XRD was used to determine the crystalline state of pure Rosuvastatin and the optimized formulation of Rosuvastatin-loaded SLN. The formulation and drug were analyzed over the angle (2Θ) range from 0^0 to 80^0 and scanned with filter Ni, Cu- Kα radiation, 20 mA current, and voltage 40 kV[20,21].

2.10.   Field emission scanning electron microscopy (FE-SEM)

The surface morphology of Rosuvastatin's optimized lyophilized SLN formulation was observed under field emission scanning electron microscopy. SEM study was conducted using Olympus Corporation FV300022. Before studying morphology, lyophilized powder samples were placed on metal stubs using double adhesive tape. Then, the nanoparticle conductive gold was used to coat the samples under the vacuum. Finally, 8-20 kV accelerating voltage was used to analyze samples [22,23].

2.11.   In vitro Drug release studies

In vitro release was conducted on calibrated dissolution test apparatus (Electrolab Mumbai, India) at 37±0.5o C. pH 6.8 phosphate buffer was used to study *in vitro* drug release of RTSLN. A 5 ml Formulation equivalent to 10 mg was placed inside the dialysis bag, which was soaked in dissolution medium last 12 hours and tied at both ends to the paddle rod. The paddle was placed in a dissolution medium with constant stirring speed. Aliquots of 5 ml dissolution medium were withdrawn every certain interval while fresh to keep sink volume constant; the dissolution medium was replaced.

UV wavelength of 242.5 nm was used to analyze the sample solution[23].

2.12.   Ex vivo absorption study

Formulation of the optimized batch of RTSLN was used to conduct an absorption study on everted chicken ileum using the ex *vivo* absorption method—U-shaped perfusion glass apparatus with 25 ml volume capacity used to tie chicken ileum. After mounting, an everted segment on the glass apparatus was filled with 25 ml thyroid solution. Now, place the assembly into the beaker having 250 ml of pH 6.8 phosphate buffer containing SLN formulation 10 ml and constant supply with aeration. Mount the assembly over a magnetic stirrer and maintain 37±0.5°C temperature. The serosal side becomes an internal part of the tube, whereas the mucosal side would be a buffer solution in the beaker. Samples for analysis were collected from the tyroid solution after every 1 hour. % permeation was assessed using UV wavelength at 242.5 nm. Replacement of the tyroid solution with a fresh one is mandatory to compensate for sampling loss[23].

2.13.   Contour plots and surface response plots

The values of the response are diagrammatic, represented using contour plots and surface response plots. It helps in explaining the relationship between independent and dependent variables. Response surface methodology (RSM) exhibits how an experimental response and a set of input variables are related. RSM sets a mathematical trend in the experimental design for determining the optimum level of experimental factors required for a given response. The reduced models were used to plot two-dimension contour plots and three dimensions RSM using Design of Expert[24,25,26,32-36].

3.   RESULTS AND DISCUSSION

3.1.   Selection of Lipid

Lipid was selected based on the highest solubility criterion of the active ingredient in lipid. GMS was found suitable as only 200 mg is required to dissolve 100 mg of Rosuvastatin, compared to stearic acid and gelucire, for the formulation of RTSLN.

Table II: Rosuvastatin Solubility in different lipids		
Lipids	Solubility	Quantity of lipid Required to dissolve 100 mg of the drug
GMS	Soluble	200
Stearic acid	Soluble	380
Gelucire	Insoluble	-

3.2.   Selection of surfactant

The choice of surfactant is based on the production of nanosized particles, smaller polydispersity index, safety, and stability. Poloxamer 407 satisfactorily complied with the characteristics stated above.

3.3.   Solubility study

Several solvents were used to check the solubility of RT and observed to be sparingly soluble in water and chloroform—freely soluble in methanol, ethanol, and phosphate buffer pH 6.8.
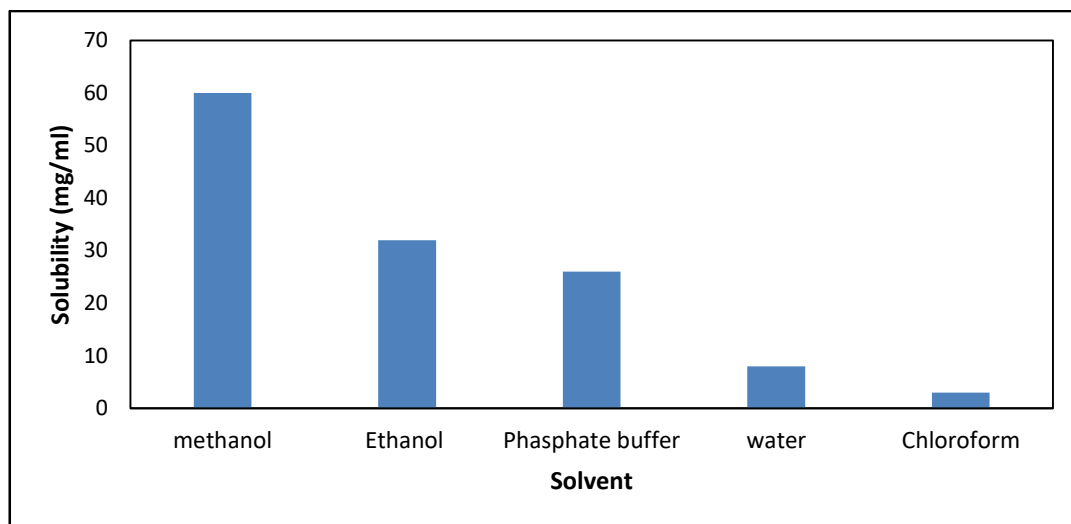
Fig I: Solubility study of Rosuvastatin in various solvents

3.4. Melting point

The melting point of RT was found to be 142- 146 °C UV visible spectrophotometer was used to prepare a standard calibration curve of RT and observed absorbance spectra at 242.5 nm. 2-10 μ g/ml concentration was used to check linearity. The correlation coefficient was observed to be 0.9950

3.5. Calibration curve

UV visible spectrophotometer was used to prepare a standard calibration curve of RT and observed absorbance spectra at 242.5 nm. In addition, 2-10 μg/ml concentration was used to check linearity. The correlation coefficient was observed at 0.9950. Fig.II depicts the absorption spectra of RT in methanol.
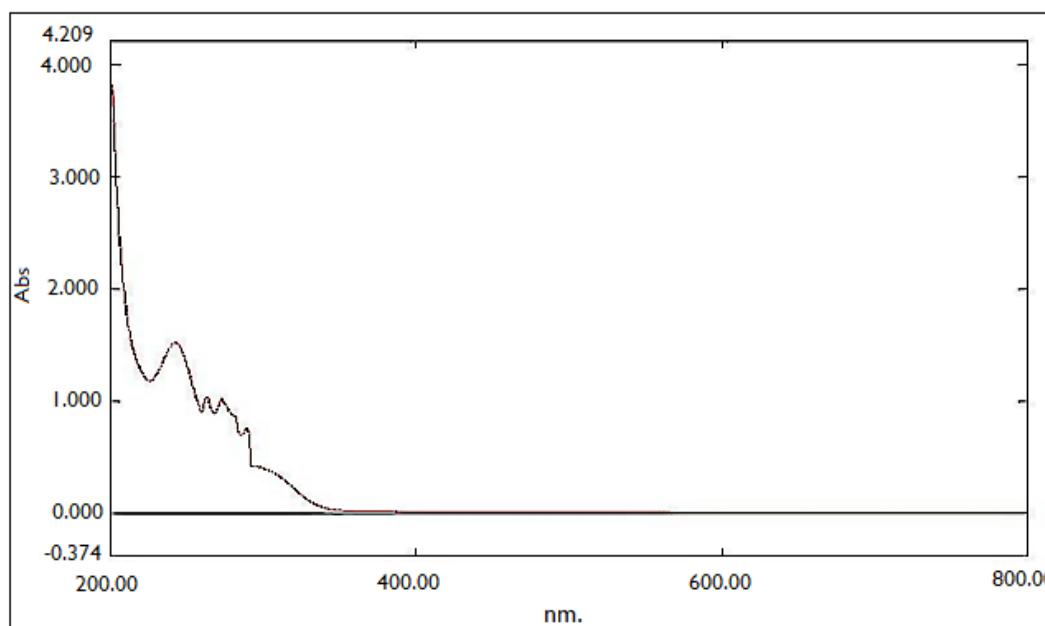

Fig II: Absorption spectra of RT

3.6. Entrapment efficiency

A 3D counter-plot from the design of expert software was used to predict the effects of the amount of GMS and concentration of poloxamer 407 on factor EE (Fig. Xb). The 13 experimental batches for EE ranged from 53% to 78%. At a higher (5%) concentration of GMS and 0.5 % concentration of poloxamer 407, the formulation has shown 78% EE. Therefore, we conclude that %EE increased with the highest concentrations of GMS and poloxamer 407.

3.7. Particle size

Table I shows the size of prepared RTSLN varied within the 254.2 to 863.4 nm ranges. A particle size increases depending on GMS and poloxamer 407 concentration. When the GMS concentration increases, particle size also increases, while the increase in poloxamer 407 concentration causes a decrease in particle size; this could be due to more solubilization of the drug in lipids. Fig. III shows the optimized batch's average particle size, which was 254.2 nm.
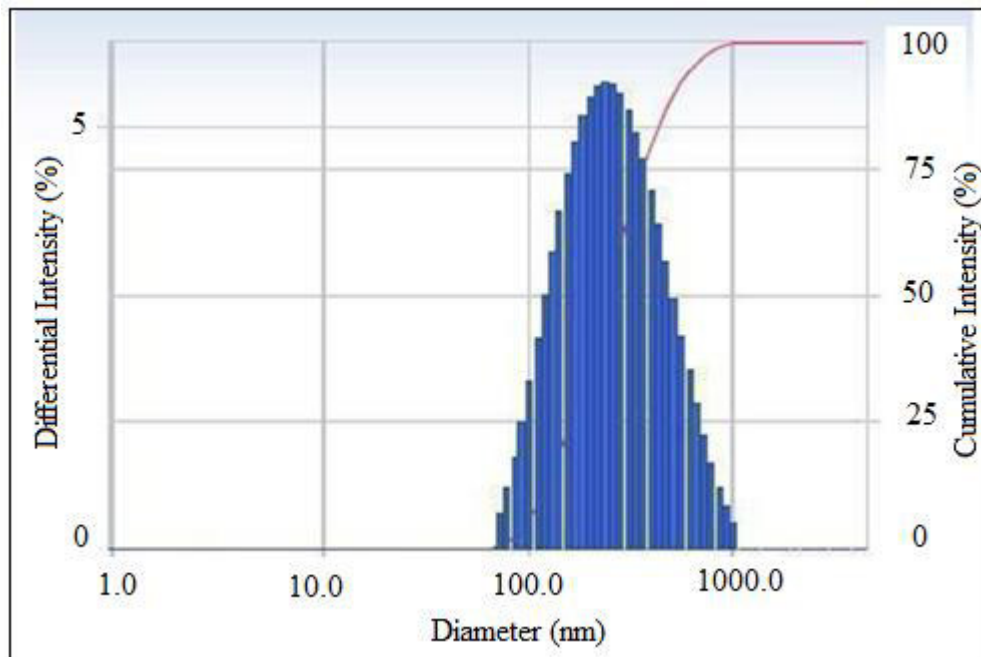
Fig III: Particle size of RTSLN formulation

3.8. Zeta potential & Polydispersity index (PDI)

The physical stability of SLN dispersion is governed by PDI, which is an important parameter for the long-term stability of SLN dispersion. Therefore, the PDI should be as low as possible, with a range of 0 to 1 defining the dispersion homogeneity. A value near 1 shows heterogeneity and less than 0.5 shows homogeneity. The PDI value for all formulations was found within the range of 0.112 to 0.478, which was less than 0.5, indicating homogeneity.

3.9. Zeta Potential

The stability of colloidal dispersions upon storage depends on Zeta potential. The repulsion effect between charged nanoparticles causes better colloidal suspension stability if a Nanoparticulate system has a larger zeta potential value. The zeta potential values have a range between -24 to -40 mV. The surfactant concentration has a potential impact on the charge of the particle. It was observed that, as the concentration of surfactant was increased from 0.5 to 1.5%, there was a decrease in the value of zeta potential. The surfactant is non-ionic, and increasing its concentration lowers the total charge on the particle. The optimized batch of Rosuvastatin Calcium loaded SLNs (Batch RT6) was found to have a Zeta potential of -34.52 ± (-2.75) mV. For well-stabilized nanoparticles, Zeta potential values must be present in the ± 15 mV to ± 50 mV Hence, it was concluded that the nanoparticles would remain stable.

Table III: Evaluation parameters of SLN batches RT1-RT13 (Mean ± SD, n=3).

Experimental Run	PDI	Zeta Potential (mV)
RT 1	0.135±0.044	-35.38±(-1.57)
RT 2	0.440±0.034	-26.04±(-2.94)
RT 3	0.321±0.009	-27.08±(-0.75)
RT 4	0.333±0.011	-28.47±(-0.94)
RT 5	0.346±0.046	-24.75±(-1.21)
RT 6	0.163±0.040	-35.31±(-1.07)
RT 7	0.436±0.016	-27.59±(-1.94)
RT 8	0.352±0.041	-26.78±(-2.31)
RT 9	0.454±0.034	-24.89±(-2.08)
RT10	0.339±0.042	-30.91±(-1.91)
RT 11	0.330±0.025	-26.60±(-0.72)
RT 12	0.352±0.046	-27.21±(-1.35)
RT 13	0.251±0.035	-29.78±(-1.68)

3.10. Data analysis of Y1 (%EE)

%EE of SLNs was determined using the ultracentrifugation method. The %EE varied from 53% to 78%. The results indicated that Y1 is strongly affected by the amount of lipid and concentration of surfactant selected (Table IV) for the study. An increase in the number of lipids leads to an increase in %EE, which could be explained by more lipids available for Rosuvastatin Calcium to dissolve. The response (Y1) obtained at various levels of two independent variables was subjected to multiple regression for a quadratic polynomial equation.

$$\%Entrapment\ Efficiency(Y1) = 63.06 + 6.5X1 + 6X12 + 0.76X22 - 1.5X1X2$$ 1

The above mentioned equation signifies a positive value for synergistic while negative values represent an antagonistic effect. ANOVA responses for model Y1 are shown in Tables IV. The quadratic equation explains how the independent variables X1, X2, X12, X22, and X1X2 affected the Entrapment (Y1). These independent variables significantly impacted EE and particle size at $P < 0.05$. Both models had F values of 4228.5 and 174.31 at $P < 0.05$, which indicated they were significant. Table VI shows the diagnostic case statistics. The model was a significantly fit as the difference between actual and predicted values was less [27,28].

3.11. *Data analysis of Y2 (particle size)*

Table I shows the mean particle sizes of all thirteen batches found in the 254.2 to 863.4 nm range. A particle size increases depending on GMS and poloxamer 407 concentration. When the GMS concentration increases, particle size also increases, while the increase in poloxamer 407 concentration causes a decrease in particle size; this could be due to more solubilization of the drug in lipids. Figure III shows the optimized batch's average particle size, which was 254.2 nm. The response (Y2) obtained at various levels of two independent variables was subjected to multiple regression for a quadratic polynomial equation.

$$Particle\ Size(Y2) = 599.12 - 173.67X1 - 132.73X2 + 26.07X1X2 - 58.41X12 + 1.79X22$$ 2

The abovementioned equation signifies a positive value for synergistic while negative values represent an antagonistic effect. ANOVA responses for model Y2 are shown in Tables IV. The quadratic equation explains how the independent variables X1, X2, X12, X22, and X1X2 affected the particle size (Y2) responses. These independent variables significantly impacted %EE and particle size at $P < 0.05$. Both models had F values of 4228.5 and 174.31 at $P < 0.05$, indicating they were significant. Table VI shows the diagnostic case statistics. The model was significantly fit as the difference between actual and predicted values was less.

3.12. *Infrared spectroscopy*

The FTIR spectra of pure drug and optimized formulation were recorded. Characteristic peak of RT was observed at 3367.82 cm^{-1} for O-H, 1604.83 cm^{-1} for C=C, 1437.02 cm^{-1} for CH$_3$ bending, 1155.40 cm^{-1} for SO$_2$, and 1508.38 cm^{-1} for NH bending. RTSLN peaks were observed at 1383.01 cm^{-1} for CH3 bending, 1739.85 cm^{-1} for C=O, and 1471.74 for C-H. The drug entrapment in the lipid matrix was confirmed from FTIR of lipid GMS and formulation RTSLN, the disappearance of the characteristic peaks of the drug, and replacement by the peak of GMS. At the same time, other peaks replaced or shifted in the IR spectra of formulation (Fig. IV).
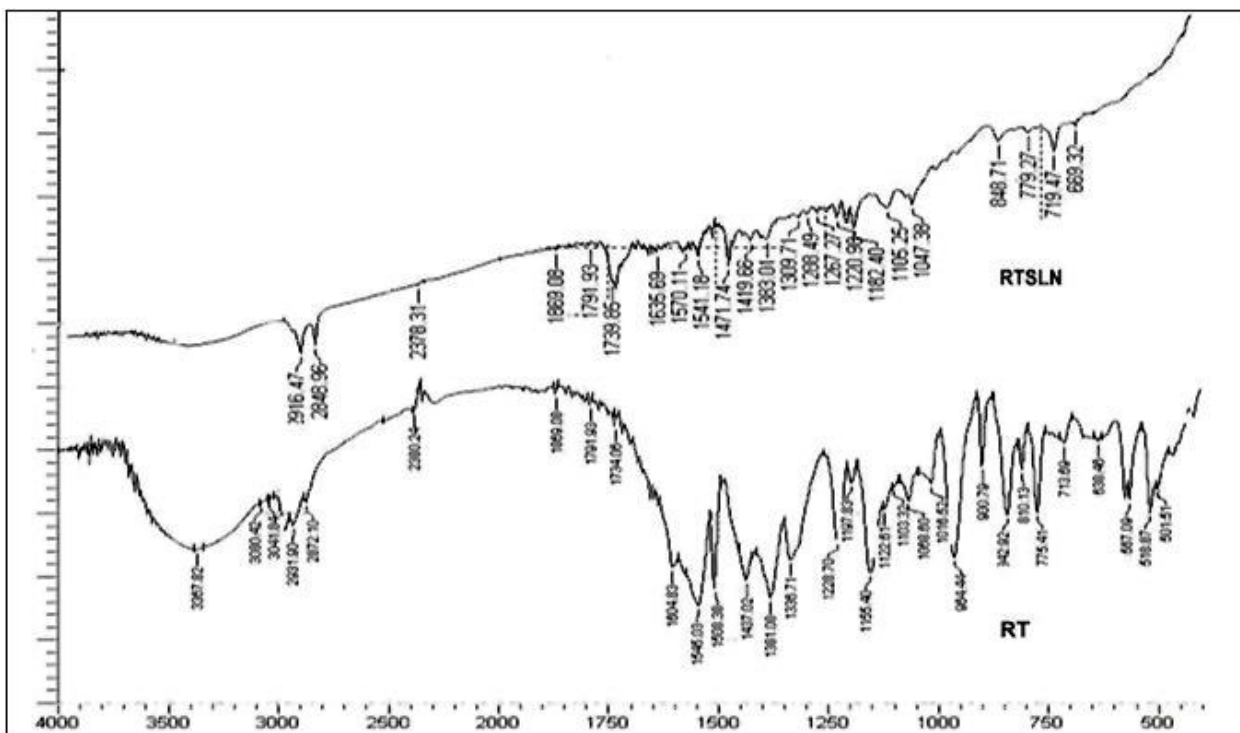

Fig IV: FTIR of RT and RTSLN formulation

3.13. Differential Scanning Calorimetry

A 60^0 C endothermic peak in the DSC analysis of the SLN formulation indicated the presence of GMS. However, in the formulation of RTSLN, there was no observable RT peak. It shows that the RT has completely dissolved in the lipid matrix of the SLN. (Fig. V).
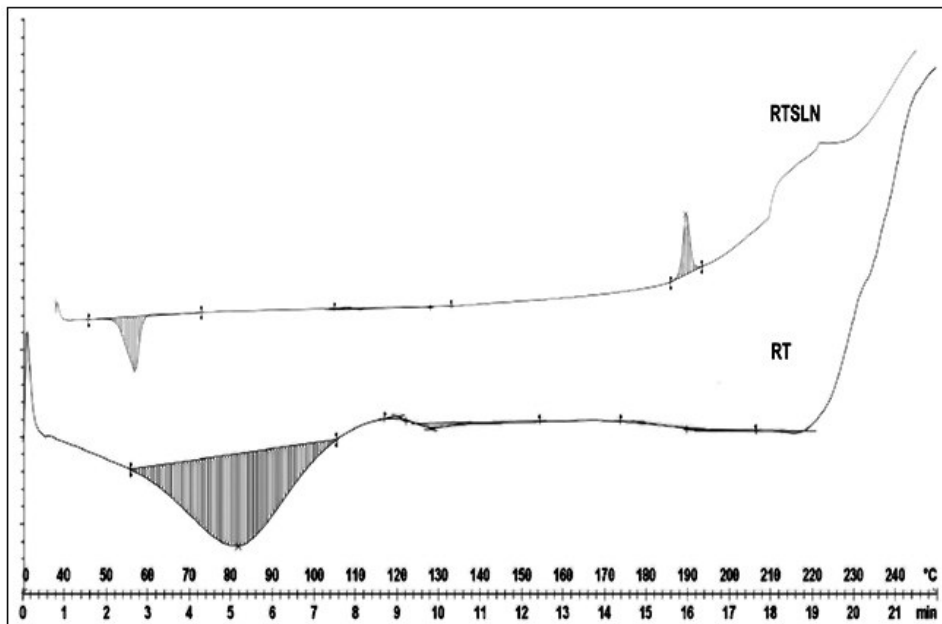

Fig V: Differential scanning calorimetry of RT and RTSLN

3.14. X-ray diffraction (XRD) analysis

Intense peaks in XRD were observed at 8.58^0, 9.08^0, 17.82^0,17.98^0,18.08^0, 18.53^0, 18.638^0, and 19.63^0,20.98^0, 21.59^0,23.1^0 indicating the crystalline nature of rosuvastatin calcium. On the other hand, the lyophilized formulation of RTSLN did not show any sharp peak characteristics of RT, which indicates its amorphous nature. This amorphization of formulation indicated a large amount of active ingredient was entrapped in the lipid and eventually dispersed homogeneously at the molecular level.
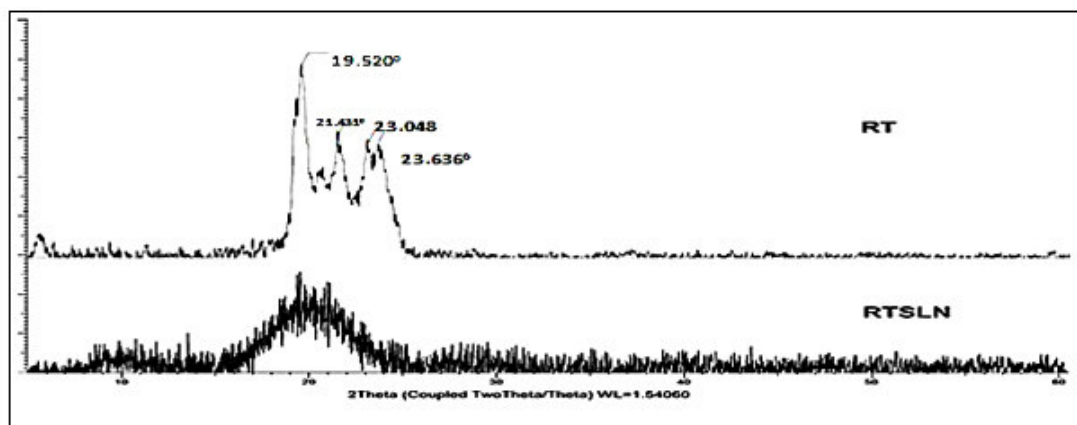

Fig VI: X-ray diffraction of RT and RTSLN

3.15. Scanning Electron Microscopy (SEM)

The SEM image showed the drug particles were irregular and non-smooth surfaces and then transformed into spherical solid lipid nanoparticles. The micrograph indicates that the optimized formulation of solid lipid nanoparticles has a sphere shape of RTSLN formulation (Fig. VII).
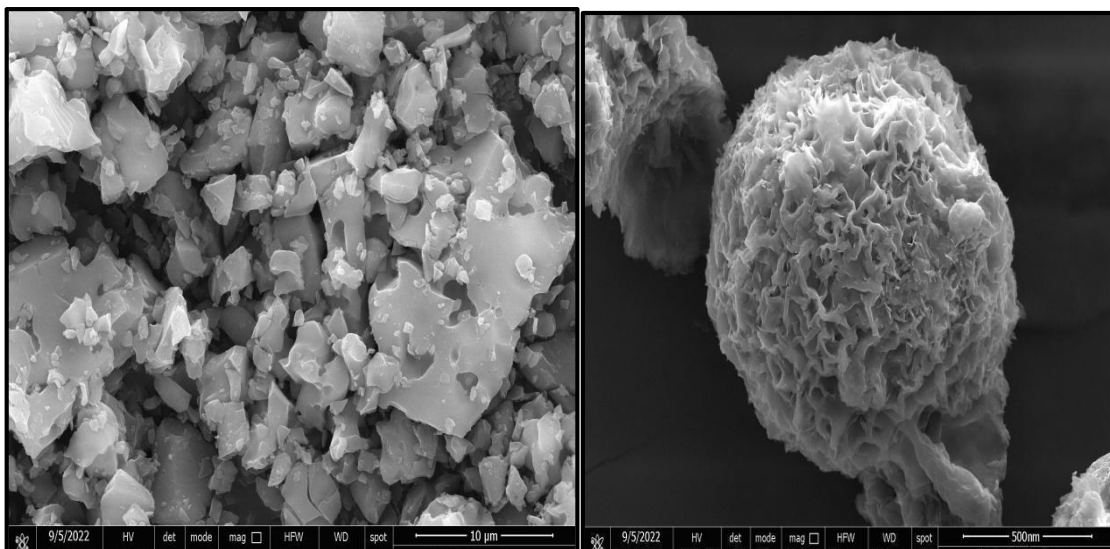
Fig VII: SEM of RT and RTSLN formulation

3.16. In vitro Drug release studies

RTSLN in vitro release was assessed using pH 6.8 phosphate buffer for 8 hours using a dialysis membrane. Optimized RTSLN batch showed 79.8 %, and pure drug RT showed 88.2% release. The initial rapid release may be due to free drugs from the SLN. Release from SLN includes a complex mechanism based on diffusion from the lipid matrix (Fig. VIII). A modified dialysis method was used to study *in vitro* drug release of Rosuvastatin Calcium loaded SLNs. Within two hours Optimized batch showed the initial rapid drug release of 15-30%, followed by sustained drug release of the remaining 30-80% upto 8hours and beyond. The preliminary fast drug release may be attributed to the diffusion of the dissolved drug, initially deposited inside the pores of the nanoparticles, and the free drug's presence in the external phase and on the surface of the nanoparticles. The reason for the sustained release of the drug from the internal lipidic phase after initial burst release is the lipophilic nature of Rosuvastatin calcium. Also, it was found that Particle size affects the drug release rate. Small-sized nanoparticles lead to a shorter average diffusion path of the Rosuvastatin entrapped and a faster release rate of the entrapped drug than bigger-size nanoparticles. The larger-sized nanoparticles could prolong the release of the drug up to 12 hours and beyond. The drug release was also affected by the concentration of surfactant and lipids. The drug release rate decreased when the lipid concentration was increased, possibly due to the large concentration of drug presence in the inner core. The drug release rate increased, as the surfactant concentration increased, due to the increased solubility of the drug in the external phase[29,30,31].
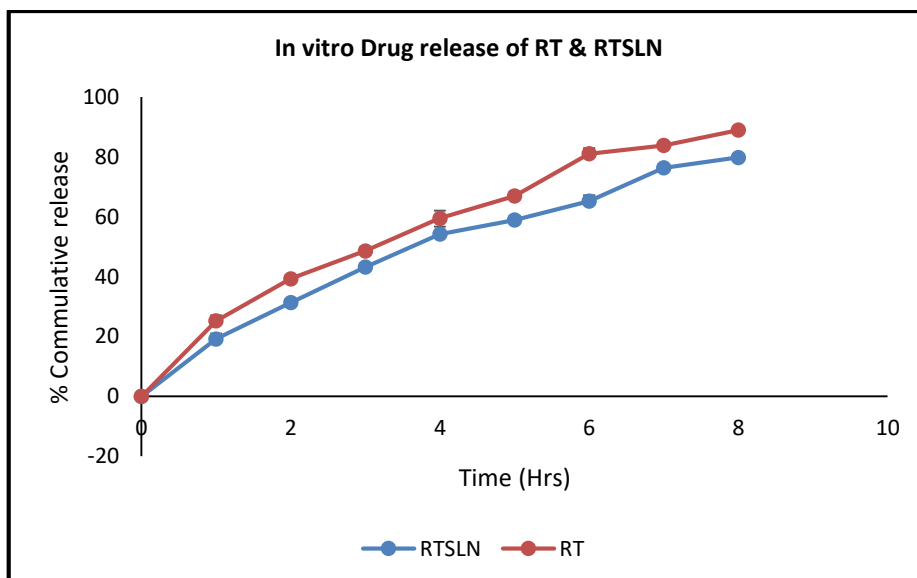

Fig VIII: In vitro drug release profile of RTSLN formulation

3.17. Ex vivo absorption study

Fig. IX shows the result of RTSLN for ex vivo absorption through everted chicken ileum. Permeation absorption for pure drug RT was 90.2%, while for an optimized batch of RTSLN was 76.7 % formulation [31].
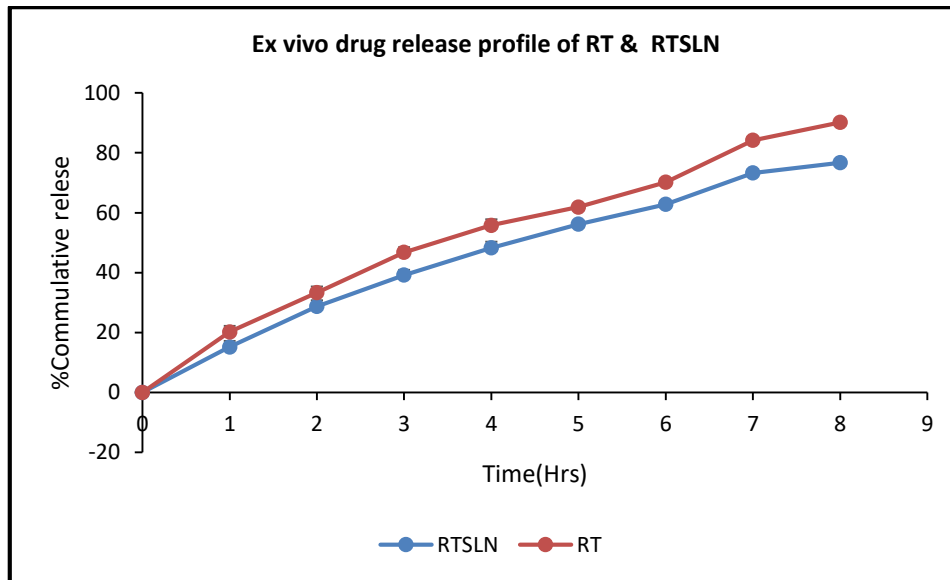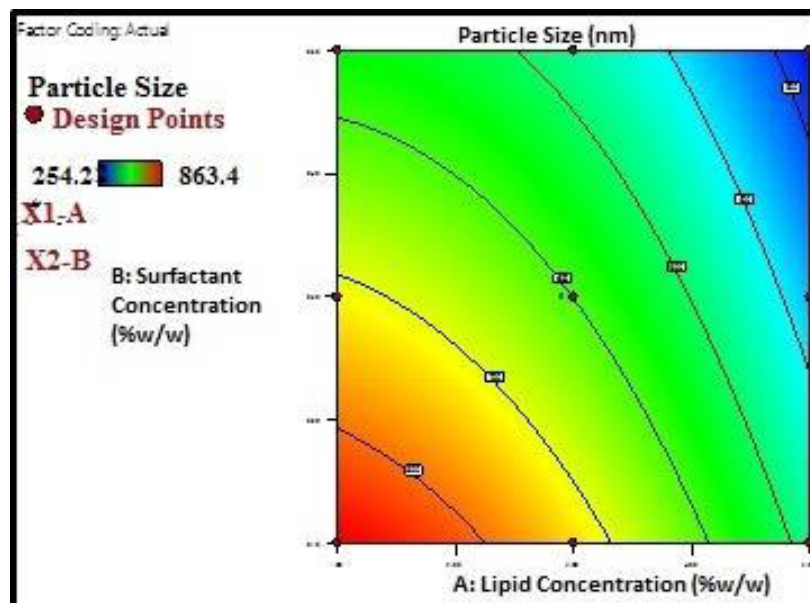
Fig IX: Ex vivo release profile of Rosuvastatin (RT) & RTSLN

3.18. Contour plots and response surface analysis

Two-dimensional contour plots and 3-D response surface plots for variables Y1 (particle size) are shown in Fig. X (a,b), respectively. Similarly, two-dimensional contour plots and 3-D response surface plots for variables Y2 (%EE) are shown in Fig. XI(a,b), respectively. They are very useful for studying the interaction, main, and quadratic effects of the factors (independent variables) on the responses (dependent variables). These types of plots help depict the study of the effects of two factors on the response at a time. Fig. IX reveals a decline in particle size with increased surfactant concentration. An increase in the number of lipids led to an increase in particle size. The smallest particle size was reported with the highest surfactant and the lowest amount of lipid.
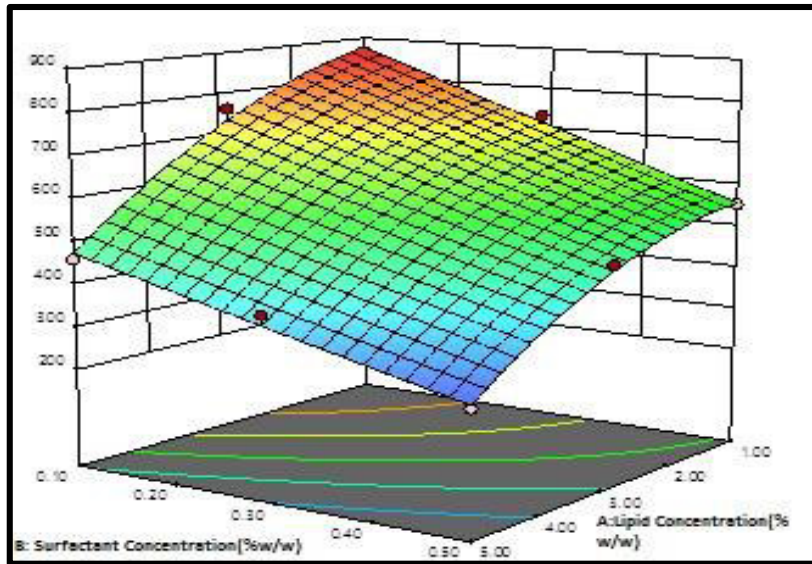
Fig X: Various plots showing the influence of GMS concentration and Poloxamer 407 concentration on the particle size a) 2D Contour plot and b) 3D Response surface plot

Fig. X indicates the effect of variables X1 & X2 on particle size (Y2) can be explained with a 2-dimensional contour plot (Fig. Xa) and 3-dimensional response surface plot (Fig Xb). GMS concentration (X1) increases particle size (Y2). An increase in Poloxamer 407 concentration (X2) showed a slight decrease in response (Y2). Fig. XI(a,b) reveals an increase in entrapment efficiency with an increase in the concentration of lipids. The highest entrapment efficiency was obtained with the highest amount of lipid.
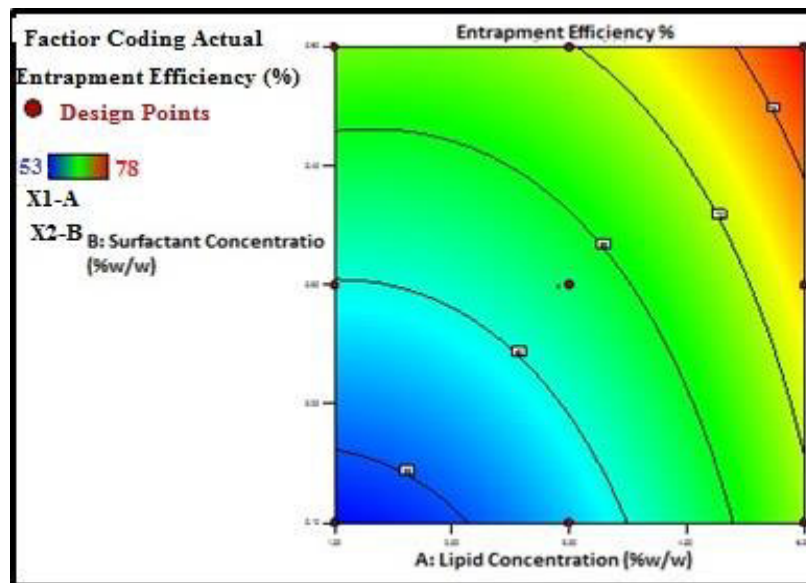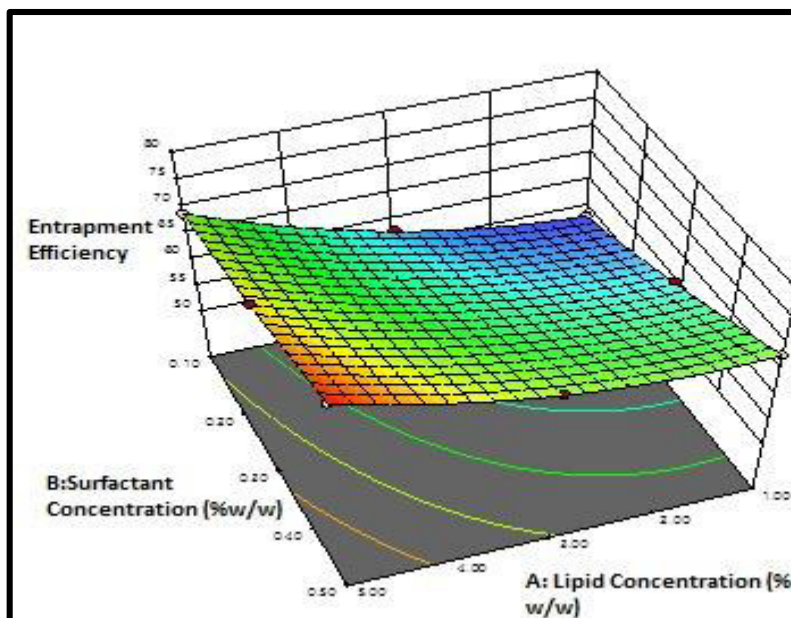
**Fig XI: Various plots showing the influence of GMS and Poloxamer 407 concentration on the % drug '
entrapment a) 2D Contour plot and b) 3D Response surface plot**

Fig. XI indicates the 2D contour plot (Fig. XIa) and 3D response surface plot (Fig. XIb) indicating the relative effect of increasing Glyceryl monostearate and poloxamer 407 concentration on % entrapment efficiency of Rosuvastatin calcium SLN (Y1). With the increase in GMS concentration (X1) and Poloxamer 407 concentration (X2), the % entrapment efficiency was increased, which can be confirmed from equation 1. At different levels (-1, 0, 1) of GMS concentration, was increased, the % The 2D and 3D graph indicates the increase in entrapment efficiency with increase in the concentration of lipid & surfactant. The orange indicates the higher entrapment efficiency region, while the blue indicates the lower entrapment efficiency region.

Table IV: Summary of results of regression analysis for response Y1 & Y2						
Model Summary Statistics: EE (Y1)						
Source	Std Dev	R²	Adjusted R²	Predicted R²	Press	
Linear	2.26	0.90	0.88	0.79	108.86	
2FI	2.17	0.91	0.89	0.64	182.85	
Quadratic	0.16	0.99	0.99	0.99	1.17	Suggested
Cubic	0.18	0.99	0.99	0.96	20.03	
Model Summary Statistics: **Particle size (Y2)**						
Source	Std Dev	R²	Adjusted R²	Predicted R²	Press	
Linear	39.88	0.94	0.93	0.87	37286.5	
2FI	38.27	0.95	0.94	0.77	67372	
Quadratic	18.55	0.99	0.98	0.94	17088.9	Suggested
Cubic	21.04	0.99	0.98	0.14	257411	

Table V: ANOVA models for Y1 and Y2						
Source	**Sum of Squares**	**DF**	**Mean square**	**F Value**	**Prob > F**	
Model for Y1						
	520.75	5	104.15	4228.5	< 0.0001	
A	253.5	1	253.5	10292.1	< 0.0001	
B	216	1	216	8769.6	< 0.0001	significant
A2	29.327586	1	29.3276	1190.7	< 0.0001	
B2	1.589491	1	1.58949	64.5333	< 0.0001	
AB	9	1	9	365.4	< 0.0001	
Model for Y2						
	300164.78	5	60033	174.31	< 0.0001	
A	180960.67	1	180961	525.46	< 0.0001	
B	105708.83	1	105709	306.95	< 0.0001	significant
A2	9422.97	1	9422.98	27.36	0.0012	
B2	8.84	1	8.84601	0.025	0.8772	
AB	2719.62	1	2719.62	7.89	0.0261	

Table VI: Diagnostics Case Statistics for response variables.							
Diagnostics Case Statistics: EE (Y1)				Diagnostics Case Statistics: Particle size (Y2)			
Standard Order	Actual Value	Predicted Value	Residual	Standard Order	Actual Value	Predicted Value	Residual
	53	53.08	-0.08	1	863.4	874.97	-11.57
2	58	57.82	0.17	2	760.4	733.64	26.78
3	69	69.08	-0.086	3	460.3	475.48	-15.18
4	60	59.82	0.17	4	730.3	714.37	15.92
5	63	63.06	-0.069	5	591.3	599.11	-7.81
6	73	72.82	0.17	6	390.2	367.04	23.15
7	68	68.08	-0.086	7	553	557.35	-4.35
8	70	69.82	0.17	8	480.5	468.17	12.32
9	78	78.08	-0.0862	9	254.2	262.17	-7.97
10	63	63.069	-0.069	10	591.3	599.11	-7.81
11	63	63.069	-0.069	11	591.3	599.11	-7.81
12	63	63.069	-0.069	12	591.3	599.11	-7.81
13	63	63.069	-0.069	13	591.3	599.11	-7.81

The data obtained were analyzed using Design of Expert software (version 13.0). Data are presented as the mean ± standard deviation (SD). Analysis of variance (ANOVA) is used to analyze data. P values < 0.05 were considered significant.

4. CONCLUSION

The RTSLN was developed successfully in the current study. The newly created RTSLN formulations exhibit an 8-hour prolonged drug release. The 3^2 where three-level and two-factor optimization was preferred to study the effects of dependent variables (EE and particle size) on the responses of independent variables (GMS and poloxamer 407). The results of %EE were in the range from 53 % to 78%, while particle size was in the range of 254.2 to 863.4 nm. *In vitro* and *ex vivo* drug release of the optimized batch was sustained, which was found to be 79.8 % and 76.7% after 8 hours, respectively. In FTIR, XRD, and DSC spectra, no interactions were reported. SEM shows the spherical SLNs. The microwave microemulsion method of formulation of SLN overcomes the drawback of conventional heating used in the microemulsion SLN formulation method. Hence, to get uniform-sized homogenous solid lipid nanoparticles, the microwave-assisted microemulsion technique in which microwave radiation is used to overcome the drawbacks associated with conventional thermal energy plays an important role.

6. AUTHORS CONTRIBUTION STATEMENT

Mr. Nilesh B Chaudhari contributed by studying the experimental part. In contrast, Dr. Amar G Zalte and Dr. Vishal S Gulecha contributed by performing a Design of Expert software study and an Ex vivo study of Rosuvastatin-loaded solid lipid nanoparticles.

7. CONFLICT OF INTEREST

Conflict of interest declared none.

8. REFERENCES

1. Rouco H, Diaz-Rodriguez P, Remunan-Lopez C, Landin M. Recent advances in solid lipid nanoparticles formulation and clinical Applications, Nanomaterials for Clinical Applications; 2020. p. 213-47.
2. Dudhipala N, Veerabrahma K. Improved anti-hyperlipidemic activity of rosuvastatin calcium via lipid nanoparticles: pharmacokinetic and pharmacodynamic evaluation. Eur J Pharm Biopharm. 2017;110:47-57. doi 10.1016/j.ejpb.2016.10.022, PMID 27810472.
3. Katkade PN. Formulation and evaluation of solid lipid nanoparticles of selected active pharmaceutical ingredients [Ph.D. thesis]; 2017.
4. Biswal S, Sahoo J, Murthy PN, Giradkar RP, Avari JG. Enhancement of dissolution rate of gliclazide using solid dispersions with polyethylene glycol 6000. AAPS PharmSciTech. 2008;9(2):563-70. doi: 10.1208/s12249-008-9079-z, PMID 18459056.
5. Chakraborty S, Shukla D, Mishra B, Singh S. Lipid–an emerging platform for oral delivery of drugs with poor bioavailability. Eur J Pharm Biopharm. 2009;73(1):1-15. doi 10.1016/j.ejpb.2009.06.001, PMID 19505572.
6. Potta SG, Minemi S, Nukala RK, Peinado C, Lamprou DA, Urquhart A, et al. Development of solid lipid nanoparticles for enhanced solubility of poorly soluble drugs. J Biomed Nanotechnol. 2010;6(6):634-40. doi 10.1166/jbn.2010.1169, PMID 21361127.
7. Mukherjee S, Ray S, Thakur RS. Solid lipid nanoparticles: A modern formulation approach in drug delivery system. Indian J Pharm Sci. 2009;71(4):349-58. doi: 10.4103/0250-474X.57282, PMID 20502539.
8. Kadam RS, Bourne DW, Kompella UB. Nano-advantage in enhanced drug delivery with biodegradable nanoparticles: contribution of reduced clearance. Drug Metab Dispos. 2012;40(7):1380-8. doi 10.1124/dmd.112.044925, PMID 22498894.
9. Yildirimer L, Thanh NT, Loizidou M, Seifalian AM. Toxicology and clinical potential of nanoparticles. Nano Today. 2011;6(6):585-607. doi: 10.1016/j.nantod.2011.10.001, PMID 23293661.

10. Dhome AG, Deshkar SS, Shirolkar SV. Gliclazide solid lipid nanoparticles formulation, optimization, and in vitro characterization. Pharm Reson. 2018;1(1):8-16.

11. Urbán-Morlán Z, Ganem-Rondero A, Melgoza-Contreras LM, Escobar-Chávez JJ, Nava-Arzaluz MG, Quintanar-Guerrero D. Preparation and characterization of solid lipid nanoparticles containing cyclosporine by the emulsification-diffusion method. Int J Nanomedicine. 2010;5:611-20. doi: 10.2147/IJN.S12125, PMID 20856836.

12. Shah RM, Eldridge DS, Palombo EA, Harding IH. Encapsulation of clotrimazole into solid lipid nanoparticles by microwave-assisted microemulsion technique. Appl Mater Today. 2016;5:118-27. doi 10.1016/j.apmt.2016.09.010.

13. Schmink JR, Leadbeater NE. Microwave heating as a tool for sustainable chemistry, Microwave heating is a tool for sustainable chemistry. CRC Press. p. 20014; 1-24.

14. Sharma S, Kanugo A, Gaikwad J. Design and development of solid lipid nanoparticles of tazarotene for treating psoriasis and acne: quality by design approach. Material technology advanced performance materials. Taylor & Francis, 2020.

15. Souza LG, Silva EJ, Martins AL, Mota MF, Braga RC, Lima EM, et al. Development of topotecan-loaded lipid nanoparticles for chemical stabilization and prolonged release. Eur J Pharm Biopharm. 2011;79(1):189-96. doi 10.1016/j.ejpb.2011.02.012, PMID 21352915.

16. Silva AC, González-Mira E, García ML, Egea MA, Fonseca J, Silva R, et al. Preparation, characterization and biocompatibility studies on risperidone-loaded solid lipid nanoparticles (SLN): high-pressure homogenization versus ultrasound. Colloids Surf B Biointerfaces. 2011;86(1):158-65. doi 10.1016/j.colsurfb.2011.03.035, PMID 21530187.

17. Chaudhari NB, Zalte AG, Gulcha VS. Advanced technologies in the preparation of solid lipid nanoparticles: a review. Journal of Seybold report. 2020;25(10):414-25.

18. Pandya BJ, Parmar RD, Soniwala MM, et al. Solid lipid nanoparticles: overview on excipients. Asian J Pharm Technol Innov. 2013;01(03):01-9.

19. Shirsath NR, Goswami AK. Vildagliptin loaded gellan gum mucoadhesive beads for sustained drug delivery: design, optimization, and evaluation. Material technology advanced performance materials. Taylor & Francis, 2020.

20. Ekambaram P, Sathali AH, Priyanka K. Solid lipid nanoparticles: a review. Sci Rev Chem Commun. 2012:80-102; Supp11.

21. Vogel's textbook of quantitative chemical analysis. 5th ed. London: ELBS Longman; 1997. p. 661-72.

22. Singh B, Sharma V, Chauhan D. Gastroretentive floating sterculia–alginate beads for antiulcer drug delivery. Chem Eng Res Des. 2010;88(8):997-1012. doi: 10.1016/j.cherd.2010.01.017.

23. Naik JB, Waghulde MR. Development of vildagliptin loaded Eudragit® microspheres by screening design: in

vitro evaluation. J Pharm Investig. 2018;48(6):627-37. doi: 10.1007/s40005-017-0355-3.

24. Dhoranwala KA, Shah P, Shah S. Formulation optimization of Rosuvastatin calcium-loaded solid lipid nanoparticles by 32 full-factorial design. Nanoworld J. 2015;1(4):112-21. doi: 10.17756/nwj.2015-015.

25. Miller JC, Miller JN. Statistics for analytical chemistry. 2nd ed. New York: Wiley; 1984. p. 83-11.

26. Indian pharmacopoeia 2007. Vol –II, Government of India, Ministry of Health and Family Welfare, The controller of publications. New Delhi:599-600.

27. British Pharmacopoeia. Department of Health London: The Stationary Office. Vol. 2009: 232, 489; I:1048-50.

28. United State Pharmacopoeia, Ville R. 31st ed, US convection INC. 2008;1193:2373.

29. Fernanda IB, Fabiola GP, Beatriz SF. Gellan gum microspheres crosslinked with trivalent ion: effect of polymer and crosslinker concentrations on drug release and mucoadhesive properties. Drug Dev Ind Pharm. 2015;42:9045-51.

30. Nayak AK, Pal D, Santra K. Artocarpus heterophyllus L. seed starch-blended gellan gum mucoadhesive beads of metformin HCl. Int J Biol Macromol. 2014;65:329-39. doi: 10.1016/j.ijbiomac.2014.01.022, PMID 24447799.

31. Patil J, Rajput R, Nemade R, Naik J. Preparation and characterization of artemether loaded solid lipid nanoparticles: a 3 2 factorial design approach. Materials Technology. 2020;35(11-12):719-26. doi 10.1080/10667857.2018.1475142.

32. Raina H, Kaur S, Jindal AB. Development of efavirenz loaded solid lipid nanoparticles: risk assessment, quality-by-design (Qbd) based optimization and physicochemical characterization. J Drug Deliv Sci Technol. 2017;39:180-91. doi: 10.1016/j.jddst.2017.02.013.

33. Shah B, Khunt D, Bhatt H, Misra M, Padh H. Application of quality by design approach for intranasal delivery of rivastigmine loaded solid lipid nanoparticles: effect on formulation and characterization parameters. Eur J Pharm Sci. 2015;78:54-66. doi: 10.1016/j.ejps.2015.07.002, PMID 26143262.

34. Priyadarsini S, Lahoti SR. Quality by design: optimization of letrozole solid lipid nanoparticle for breast cancer. Ind J Pharm Edu Res. 2022;56(4):1013-24. doi: 10.5530/ijper.56.4.182.

35. Agrawal Y, Patil K, Mahajan H, Potdar M, Joshi P, Nakhate K et al. In vitro and in vivo characterization of entacapone-loaded nanostructured lipid carriers developed by quality-by-design approach. Drug Deliv. 2022;29(1):1112-21. doi: 10.1080/10717544.2022.2058651, PMID 35380091.

36. Sharma S, Kanugo A, Gaikwad J. Design and development of solid lipid nanoparticles of tazarotene for treating psoriasis and acne: A quality by design approach. Mater Technol. 2022;37(8):735-44. doi: 10.1080/10667857.2021.1873637.